JACS
JOURNAL OF THE AMERICAN CHEMICAL SOCIETY

COMMUNICATION

pubs.acs.org/JACS

Poly(3-alkylthiophene) Diblock Copolymers with Ordered Microstructures and Continuous Semiconducting Pathways

Victor Ho,[†,§] Bryan W. Boudouris,[†,§] Bryan L. McCulloch,[†] Christopher G. Shuttle,[‡] Martin Burkhardt,[‡] Michael L. Chabinyc,[‡] and Rachel A. Segalman*[,†]

[†]Department of Chemical and Biomolecular Engineering, University of California, Berkeley and Materials Science Division, Lawrence Berkeley National Laboratory, Berkeley, California 94720, United States

[‡]Materials Department, University of California, Santa Barbara, California 93106-5050, United States

Supporting Information

ABSTRACT: Conjugated rod−coil diblock copolymers self-assemble due to a balance of liquid crystalline (rod−rod) and enthalpic (rod−coil) interactions. Previous work has shown that while classical block copolymers self-assemble into a wide variety of nanostructures, when rod−rod interactions dominate self-assembly in rod−coil block copolymers, lamellar structures are preferred. Here, it is demonstrated that other, potentially more useful, nanostructures can be formed when these two interactions are more closely balanced. In particular, hexagonally packed polylactide (PLA) cylinders embedded in a semiconducting poly(3-alkylthiophene) (P3AT) matrix can be formed. This microstructure has been long-sought as it provides an opportunity to incorporate additional functionalities into a majority phase nanostructured conjugated polymer, for example in organic photovoltaic applications. Previous efforts to generate this phase in polythiophene-based block copolymers have failed due to the high driving force for P3AT crystallization. Here, we demonstrate that careful design of the P3AT moiety allows for a balance between crystallization and microphase separation due to chemical dissimilarity between copolymer blocks. In addition to hexagonally packed cylinders, P3AT−PLA block copolymers form nanostructures with long-range order at all block copolymer compositions. Importantly, the conjugated moiety of the P3AT−PLA block copolymers retains the crystalline packing structure and characteristic high time-of-flight charge transport of the homopolymer polythiophene ($\mu_h \sim 10^{-4}$ cm^2 V^{-1} s^{-1}) in the confined geometry of the block copolymer domains.

While there is significant interest in using block copolymer self-assembly strategies to achieve nanoscale patterning in conjugated polymers for optoelectronics, and organic photovoltaics[1−4] specifically, the thermodynamics of self-assembly of these materials is more complicated than classical block copolymers due to the rigidity of the conjugated constituent moiety and the necessity of crystallinity to attain high charge mobility. The phase space of model conjugated block copolymers based on poly(phenylene vinylene) derivatives is at least four-dimensional, relying on the Flory−Huggins interaction parameter (χN), the volume fraction of each rod-like block (φ_{rod}), the Maier−Saupé parameter (μN), and the block length ratio ($\nu = R_{g,coil}/L_{rod}$).[1,5] Furthermore, while poly(3-hexylthiophene) (P3HT) is widely studied and of specific utility in photovoltaic applications due its high hole mobility ($\mu_h \sim 10^{-2}$ cm^2 V^{-1} s^{-1} in thin film transistors),[6−8] thermal self-assembly is generally precluded by crystallization of P3HT ($T_m \approx 220$ °C).[9−11] The P3HT moiety crystallizes as long, semiconducting wire-like domains, and the second block is forced into the amorphous domains between the P3HT fibers.[12−14] This inability to control the orientation and geometry of the semiconducting wires has led to limited utility. When specific solvent annealing conditions are used, lamellar and hexagonally packed microstructures have been observed in P3HT-based block copolymers but only when the majority component was the insulating moiety.[15]

Modifications of P3HT's chemical structure result in the ability to control rod−rod interactions and may be used to control the

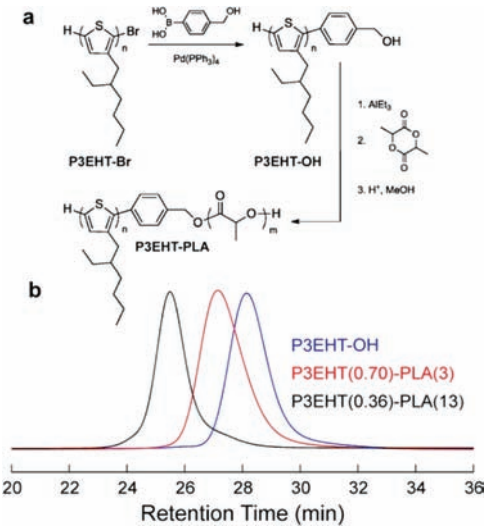

Figure 1. (a) Synthetic scheme for P3EHT−PLA using two controlled polymerization techniques. (b) SEC traces of a P3EHT−OH homopolymer and representative block copolymers. The SEC traces were taken with THF at 35 °C as the eluent at a flow rate of 1 mL min^{-1}.

Received: April 17, 2011
Published: May 24, 2011

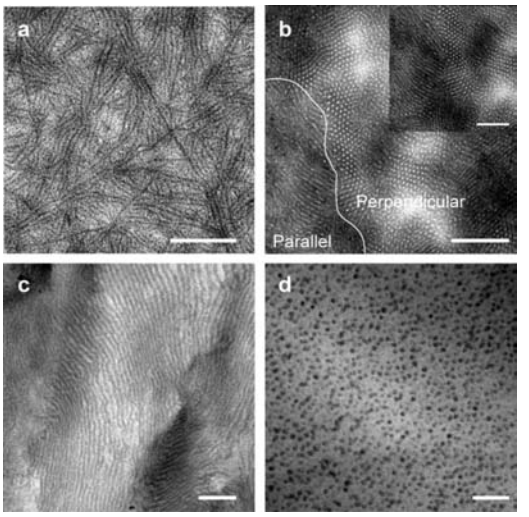

Figure 2. TEM images of (a) unstained P3EHT−OH nanofibrils (natural contrast occurs due to higher electron density in the crystalline regions) and the stained microstructures of the (b) hexagonally packed P3EHT(0.70)−PLA(3), (c) lamellar P3EHT(0.50)−PLA(7), and (d) disordered micelles of P3EHT(0.12)−PLA(56). Bulk TEM samples were annealed at 150 °C for 48 h under high vacuum and thinly sliced (∼70 nm) using a microtome. (b) TEM showing highlights of two distinct grains. In one, the long axes of the PLA cylinders are parallel to the plane of the image, and in the other the long axes of the cylinders are perpendicular to the plane of the image. The inset of (b) is a magnification showing this parallel-to-perpendicular grain boundary. The P3EHT moiety was stained dark in the block copolymer samples by exposing the samples to RuO_4 vapors for 30−50 min. All scale bars represent 200 nm.

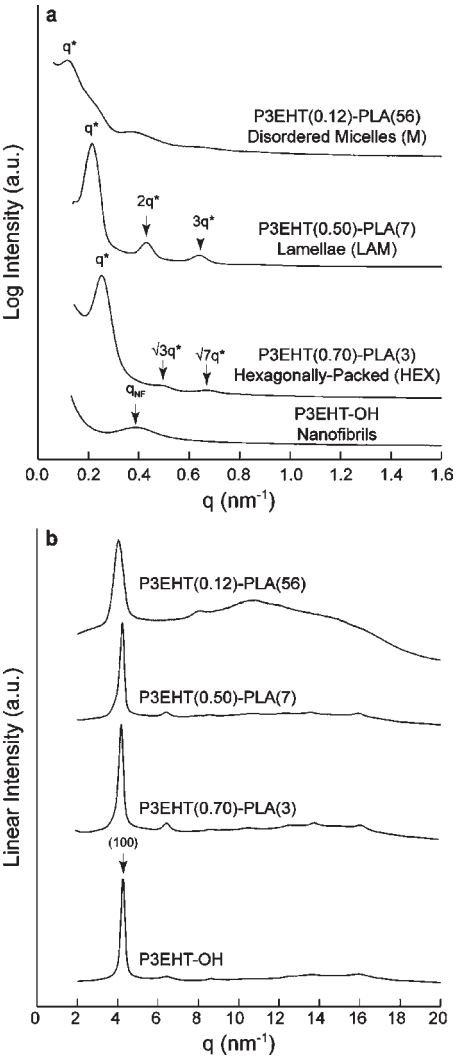

Figure 3. (a) SAXS and (b) WAXS 1D azimuthally integrated spectra for the P3EHT−OH homopolymer and representative P3EHT−PLA block copolymers for each of the three observed microstructures, HEX, LAM, and M. The bulk samples were annealed at 150 °C for 48 h under high vacuum prior to data acquisitions. The P3EHT moiety of the block copolymers remains semicrystalline at all block copolymer compositions as evidenced by the alkyl-chain stacking (100) reflections in the WAXS spectra. All spectra shown were acquired at T = 50 °C.

self-assembly of related block copolymers. For example, poly(3-(2′-ethyl)-hexylthiophene) (P3EHT) has a relatively low melting temperature ($T_m \approx 80$ °C) and rod−rod interactions that are significantly depressed relative to those of P3HT while retaining optoelectronic properties similar to those of P3HT.[16] In this work we demonstrate that poly(3-(2′-ethyl)-hexylthiophene)-*b*-polylactide (P3EHT−PLA) rod−coil block copolymers self-assemble into a number of well-ordered microstructures over the entire block copolymer composition window. Importantly, microstructures where hexagonally packed cylinders of PLA are embedded in a continuous semiconducting P3EHT matrix are observed.

P3EHT−PLA block copolymers are readily generated using a change-of-mechanism polymerization (CHOMP) scheme that utilizes two controlled polymerization techniques (Figure 1a).[17,18] These block copolymers have tunable molecular weights and narrow molecular weight distributions ($M_w/M_n \leq 1.21$) and contain no residual P3EHT homopolymer (Figure 1b), which allows for self-assembly into a number of well-ordered microstructures (Figures 2 and 3). The Grignard metathesis (GRIM) route[19,20] is used to polymerize bromine-terminated P3EHT, which is then end-functionalized with a hydroxyl group through a Suzuki coupling reaction to form the P3EHT−OH macroinitiator. Subsequent controlled ring-opening polymerization of D,L-lactide using triethylaluminium ($AlEt_3$) completes the synthesis of the P3EHT−PLA block copolymers.[21] Molecular characterization data (representative ^{1}H NMR and additional SEC traces) are shown in the Supporting Information. PLA is a desirable coil block as it not only is an amorphous material with an easily accessible glass transition temperature but also has been shown to be selectively etchable from a P3AT matrix,[22,23] suggesting opportunities to backfill the ordered, porous nanostructures with a material of complementary functionality.[24]

At high P3EHT content ($0.63 \leq w_{P3EHT} \leq 0.75$), hexagonally packed cylinders of PLA embedded in a P3EHT matrix (HEX) are observed both in bulk transmission electron microscopy (TEM) images (Figure 2b) and bulk small-angle X-ray scattering (SAXS) spectra (Figure 3a). Note that this and the other regularly ordered morphologies (Figure 2c) can be observed both at elevated temperatures (above the melting temperature of P3EHT) and upon quenching to room temperature where P3EHT is crystalline and PLA is glassy (Table 1). This is in stark contrast to the nanofibril bulk microstructure observed for the P3EHT−OH homopolymer (Figure 2a), which has a characteristic fiber width of ∼16 nm (measured from SAXS data) and is not observed above the melting temperature of P3EHT. However, crystallization of the P3EHT moiety occurs in the nanostructured block copolymer

dx.doi.org/10.1021/ja2035317 |*J. Am. Chem. Soc.* 2011, 133, 9270–9273

Table 1. Summary of P3EHT−PLA Polymer Sample Characteristics

Sample[a]	M_n[b] (kg/mol) P3EHT	M_n[b] (kg/mol) PLA	M_w/M_n[c]	w_{P3EHT}[d]	T_g (°C) PLA[e]	T_m (°C) P3EHT[e]	structure[g]	d (nm)[h]
P3EHT−OH	7.4	–	1.06	1.00	–	79	–	–
P3EHT(0.75)−PLA(2)	7.0	2.4	1.07	0.75	34	94	HEX	19.0
P3EHT(0.70)−PLA(3)	7.4	3.2	1.06	0.70	33	90	HEX	21.1
P3EHT(0.67)−PLA(4)	7.0	3.5	1.08	0.67	36	90	HEX	21.4
P3EHT(0.63)−PLA(4)	7.0	4.1	1.05	0.63	36	90	HEX	24.9
P3EHT(0.50)−PLA(7)	7.0	7.1	1.09	0.50	39	89	LAM	29.0
P3EHT(0.47)−PLA(8)	7.0	8.0	1.12	0.47	41	90	LAM	31.3
P3EHT(0.36)−PLA(13)	7.4	13.0	1.09	0.36	46	95	LAM	36.1
P3EHT(0.31)−PLA(16)	7.4	16.5	1.11	0.31	49	96	LAM	36.8
P3EHT(0.29)−PLA(17)	7.0	17.1	1.12	0.29	47	90	LAM	37.1
P3EHT(0.25)−PLA(21)	7.0	20.6	1.13	0.25	46	90	LAM	40.2
P3EHT(0.12)−PLA(56)	7.4	55.6	1.21	0.12	51	[f]	M	52.1

[a] P3EHT−OH is a homopolymer of the poly(3-(2′-ethyl)-hexylthiophene)-*b*-polylactide series symbolized by P3EHT(X)−PLA(Y) where the block copolymer is composed of X weight fraction P3EHT and has a PLA block with M_n of Y kg/mol. [b] As determined by ^{1}H NMR spectroscopy. [c] As determined by SEC versus polystyrene standards. [d] $w_{P3EHT} = M_n(P3EHT)/[M_n(PLA) + M_n(P3EHT)]$. [e] As determined by DSC at a heating rate of 10 °C min^{-1} under a nitrogen purge. [f] The P3EHT melting temperature for this sample was not prominent enough to be observed in DSC. [g] Morphology (HEX = hexagonally packed cylinders of PLA in a P3EHT matrix, LAM = lamellae, and M = P3EHT micelles in a PLA matrix) was determined by SAXS experiments at T = 50 °C. [h] The domain spacing (d) was determined from the principle reflection (q^*) acquired in SAXS experiments at T = 50 °C.

domains, which is important for the optoelectronic properties of the P3AT moiety. This is evidenced via diffraction (Figure 3b), electronic properties (Figure S6), and calorimetry (Figure S2).

The TEM image of the P3EHT(0.70)−PLA(3) block copolymer shows that hexagonally packed domains form large areas (~1 μm) of mono-orientation with large grains of PLA cylinders (P3EHT is stained dark selectively with RuO_4) running with their long axes parallel and perpendicular to the plane of the TEM image. In fact, a grain boundary is evident in Figure 2b and marked by a white line. As with other rod−coil block copolymer systems, there exists a large region of compositions ($0.25 \le w_{P3EHT} \le 0.50$) for the P3EHT−PLA system where lamellar structures (LAM) are present (Table 1) because the lamellar interfaces are generally stabilized by rod−rod interactions.[25,26]

The rigidity of the conjugated P3EHT moiety does not allow for the facile generation of microstructures with curved interfaces. Therefore, disordered micelles with spherical shapes (Figure 2d) only are observed at extremely high PLA content ($w_{P3EHT} = 0.12$). The long-range order of the LAM is confirmed both through microscopy (Figure 2c) and by the integer reflections present in the SAXS spectra. Furthermore, we note the domain spacings for LAM scale linearly with increasing coil length (Figure S4) and demonstrate the inability of the conjugated polymer to alter its chain shape, in agreement with previous reports.[27,28] In addition to forming ordered microstructures at almost all P3EHT weight fractions studied ($0.25 \le w_{P3EHT} \le 0.70$), the P3EHT domains remain semicrystalline as evidenced by the powder wide-angle X-ray scattering (WAXS) spectra (Figure 3b) and differential scanning measurements (DSC) scans (Table 1 and Figure S2). This is of crucial importance when these molecules are used in organic electronic devices as crystallinity is inherently tied to the optoelectronic properties of polymer semiconductors.[29−32] Furthermore, the intensity and breadth of the diffraction peaks change in the block copolymer. The increased intensity of the (010) reflection is significant, suggesting an increase in the correlation of $\pi-\pi$ interactions, which is directly related to the optical and charge transport properties in organic electronic devices. Finally, we note that, for the disordered micelles microstructure, a large amorphous halo associated with the PLA block appears for larger q values ($8 \le q \le 18$ nm^{-1}). The ordered HEX and LAM microstructures are present both in the solid state and when heated into the melt, and heating scans show clear endotherms which are significantly increased in block copolymer samples relative to the parent P3EHT homopolymer (Table 1). This increased thermal stability of crystalline domains has been observed previously in rod−coil block copolymers and can been attributed to pinning the rod−block at the block copolymer interface, which decreases the conformational entropy gained during melting.[33] This confinement also facilitates crystallization of the P3EHT block by providing a common nucleation point for lattice growth, as has been previously observed in PPV-based block copolymers.[34]

The bulk hole mobility in the P3EHT−PLA block copolymers was measured by time-of-flight (TOF) (Figure S6) and is comparable to those of the P3EHT and P3HT homopolymers (M_n(P3HT) ≈ 7 kg/mol) of similar molecular weights ($\mu_h \approx 10^{-4}$ cm^2 V^{-1} s^{-1}), consistent with previous results both in pristine P3AT films and in polymer−fullerene and polymer−polymer blends.[35−37] This is a direct result of the preservation of the P3AT crystal structure within the block copolymer domains and demonstrates the availability of a continuous transport pathway through the copolymer film. Consequently, the mobilities for representative HEX [P3EHT(0.75)−PLA(2), P3EHT(0.67)−PLA(4)] and LAM [P3EHT(0.47)−PLA(8)] P3EHT−PLA block copolymers show the same charge transport values with hole mobilities of $\mu_h \approx 10^{-4}$ cm^2 V^{-1} s^{-1}. These data demonstrate that, by controlling the rod−rod interactions and crystallization behavior in poly(3-alkythiophene) derivatives, well-ordered block copolymer microstructures can be generated. Additionally, we are able to control the nanoscale phase separation of the P3EHT domains while retaining the charge transport properties of the most oft-used semiconducting polymer.

In conclusion, we have synthesized a series of P3EHT−PLA rod−coil block copolymers, using polymerization techniques such that the polymers have controllable molecular weights and compositions with narrow molecular weight distributions. The use of a poly(3-alkylthiophene) derivative with a lowered crystallization temperature led to the self-assembly of the

P3EHT−PLA rod−coil block copolymers. Importantly, these form microstructures where the P3EHT block serves as the majority phase. We also observed an increase in melting temperature and diffraction peak intensity in P3EHT−PLA block copolymers where the conjugated polymer is the majority phase. These data are consistent with confinement of the crystalline P3EHT domains to the nanoscopic length scale which decreases the conformational entropy gained by melting. Because the P3EHT domains remain semicrystalline, the block copolymers can self-assemble on the 10-nm length scale while retaining the high charge transport properties commonly associated with poly(3-alkylthiophenes).

■ ASSOCIATED CONTENT

Supporting Information. Detailed synthetic procedures, experimental techniques, representative ^{1}H NMR spectra, additional SEC traces, representative DSC thermograms, SAXS data as a function of temperature, lamellar microstructure domain spacing data, additional and enlarged TEM images, and time-of-flight (TOF) mobility data. This material is available free of charge via the Internet at http://pubs.acs.org.

■ AUTHOR INFORMATION

Corresponding Author
segalman@berkeley.edu.

Author Contributions
§These authors contributed equally to this work.

■ ACKNOWLEDGMENT

We gratefully acknowledge support through an NSF CAREER award for the synthesis of the diblock copolymers. Work on materials characterization was supported by the U.S. Department of Energy under Contract No. DE-AC02-05CH11231. Parts of the X-ray scattering studies were carried out at the Advanced Light Source (ALS) on Beamline 7-3-3. The Advanced Light Source is supported by the U.S. Department of Energy under Contract No. DE-AC02-05CH11231. Additional X-ray scattering studies were carried out at the Stanford Synchrotron Radiation Laboratory (SSRL), a national user facility operated by Stanford University on behalf of the U.S. Department of Energy on Beamline 1-4. V.H. acknowledges the National Science Foundation for a graduate fellowship. B.L.M. acknowledges partial support from the Dow Advanced Materials graduate fellowship. C.S., M.G.B., and M.L.C. are supported as part of the Center for Energy Efficient Materials, an Energy Frontier Research Center funded by the U.S. Department of Energy under Award Number DE-SC0001009.

■ REFERENCES

(1) Olsen, B. D.; Segalman, R. A. *Mat. Sci. Eng. R-Rep* **2008**, *62*, 37.
(2) Segalman, R. A.; McCulloch, B.; Kirmayer, S.; Urban, J. J. *Macromolecules* **2009**, *42*, 9205.
(3) Botiz, I.; Darling, S. B. *Mater. Today* **2010**, *13*, 42.
(4) Darling, S. B. *Energy Environ. Sci.* **2009**, *2*, 1266.
(5) Olsen, B. D.; Shah, M.; Ganesan, V.; Segalman, R. A. *Macromolecules* **2008**, *41*, 6809.
(6) McCullough, R. D. *Adv. Mater.* **1998**, *10*, 93.
(7) Osaka, I.; McCullough, R. D. *Acc. Chem. Res.* **2008**, *41*, 1202.
(8) Peet, J.; Heeger, A. J.; Bazan, G. C. *Acc. Chem. Res.* **2009**, *42*, 1700.
(9) Iovu, M. C.; Craley, C. R.; Jeffries-EL, M.; Krankowski, A. B.; Zhang, R.; Kowalewski, T.; McCullough, R. D. *Macromolecules* **2007**, *40*, 4733.
(10) Iovu, M. C.; Jeffries-EL, M.; Zhang, R.; Kowalewski, T.; McCulloch, R. D. *J. Macromol. Sci., Chem.* **2006**, *43*, 1991.
(11) Higashihara, T.; Ohshimizu, K.; Hirao, A.; Ueday, M. *Macromolecules* **2008**, *41*, 9505.
(12) Li, Z. C.; Ono, R. J.; Wu, Z. Q.; Bielawski, C. W. *Chem. Commun.* **2011**, *47*, 197.
(13) Wu, Z. Q.; Ono, R. J.; Chen, Z.; Li, Z. C.; Bielawski, C. W. *Polym. Chem.* **2011**, *2*, 300.
(14) Wu, Z. Q.; Ono, R. J.; Chen, Z.; Bielawski, C. W. *J. Am. Chem. Soc.* **2010**, *132*, 14000.
(15) Dai, C. A.; Yen, W. C.; Lee, Y. H.; Ho, C. C.; Su, W. F. *J. Am. Chem. Soc.* **2007**, *129*, 11036.
(16) Ho, V.; Boudouris, B. W.; Segalman, R. A. *Macromolecules* **2010**, *43*, 7895.
(17) Schmidt, S. C.; Hillmyer, M. A. *Macromolecules* **1999**, *32*, 4794.
(18) Hillmyer, M. A. *Curr. Opin. Solid State Mater. Sci.* **1999**, *4*, 559.
(19) Loewe, R. S.; Khersonsky, S. M.; McCullough, R. D. *Adv. Mater.* **1999**, *11*, 250.
(20) Loewe, R. S.; Ewbank, P. C.; Liu, J.; Zhai, L.; McCullough, R. D. *Macromolecules* **2001**, *34*, 4324.
(21) While complete functionalization of the P3EHT−OH parent homopolymer is unlikely, residual P3EHT is removed from P3EHT−PLA by selective precipitation in petroleum ether.
(22) Boudouris, B. W.; Frisbie, C. D.; Hillmyer, M. A. *Macromolecules* **2008**, *41*, 67.
(23) Boudouris, B. W.; Frisbie, C. D.; Hillmyer, M. A. *Macromolecules* **2010**, *43*, 3566.
(24) Botiz, I.; Darling, S. B. *Macromolecules* **2009**, *42*, 8211.
(25) Olsen, B. D.; Segalman, R. A. *Macromolecules* **2005**, *38*, 10127.
(26) Olsen, B. D.; Shah, M.; Ganesan, V.; Segalman, R. A. *Macromolecules* **2008**, *41*, 6809.
(27) Pryamitsyn, V.; Ganesan, V. *J. Chem. Phys.* **2004**, *120*, 5824.
(28) Olsen, B. D.; Segalman, R. A. *Macromolecules* **2007**, *40*, 6922.
(29) Mcculloch, I.; Heeney, M.; Bailey, C.; Genevicius, K.; Macdonald, I.; Shkunov, M.; Sparrowe, D.; Tierney, S.; Wagner, R.; Zhang, W. M.; Chabinyc, M. L.; Kline, R. J.; Mcgehee, M. D.; Toney, M. F. *Nat. Mater.* **2006**, *5*, 328.
(30) Zhang, R.; Li, B.; Iovu, M. C.; Jeffries-EL, M.; Sauve, G.; Cooper, J.; Jia, S. J.; Tristram-Nagle, S.; Smilgies, D. M.; Lambeth, D. N.; McCullough, R. D.; Kowalewski, T. *J. Am. Chem. Soc.* **2006**, *128*, 3480.
(31) Lunt, R. R.; Benziger, J. B.; Forrest, S. R. *Adv. Mater.* **2010**, *22*, 1233.
(32) Street, R. A.; Northrup, J. E.; Salleo, A. *Phys. Rev. B* **2005**, 71.
(33) Olsen, B. D.; Alcazar, D.; Krikorian, V.; Toney, M. F.; Thomas, E. L.; Segalman, R. A. *Macromolecules* **2008**, *41*, 58.
(34) Olsen, B. D.; Alcazar, D.; Krikorian, V.; Toney, M. F.; Thomas, E. L.; Segalman, R. A. *Macromolecules* **2008**, *41*, 58.
(35) Mauer, R.; Kastler, M.; Laquai, F. *Adv. Funct. Mater.* **2010**, *20*, 2085.
(36) Kreouzis, T.; Kumar, A.; Baklar, M. A.; Scott, K.; Stingelin-Stutzmann, N. *Adv. Mater.* **2009**, *21*, 4447.
(37) Ballantyne, A. M.; Chen, L.; Dane, J.; Hammant, T.; Braun, F. M.; Heeney, M.; Duffy, W.; McCulloch, I.; Bradley, D. D. C.; Nelson, J. *Adv. Funct. Mater.* **2008**, *18*, 2373.